The Asp285 Variant of DNA Polymerase Beta Extends Mispaired Primer Termini via Increased Nucleotide Binding

Drew L. Murphy,[†] Jessica Kosa,[‡,#] Joachim Jaeger,[‡] and Joann B. Sweasy*[,†]

Department of Therapeutic Radiology and Department of Genetics, Yale University School of Medicine, New Haven, Connecticut 06520, and Center for Medical Sciences, Wadsworth Center, NYS-DOH, Albany, New York 12201-0509

Received October 18, 2007; Revised Manuscript Received April 16, 2008

ABSTRACT: Endogenous DNA damage occurs at a rate of at least 20,000 lesions per cell per day. Base excision repair (BER) is a key pathway for maintaining genome stability. Several pol β variants were identified as conferring resistance to 3′-azido-3′-deoxythymidine (AZT) in *Escherichia coli* (Kosa et al. (1999) *J. Biol. Chem. 274*, 3851–3858). Detailed biochemical studies on one of these AZT-resistant variants, His285 to Asp, have shown that the H285D variant of pol β possesses pre-steady-state kinetics that are similar to the wild-type polymerase. In gap filling assays with 5-bp gapped DNA, H285D showed a slight mutator phenotype. In depth single turnover kinetic analysis revealed that H285D is much more efficient than wild-type pol β at extending mispaired primer termini. This mispair extension property of H285D is attributed to a greatly increased binding to the next correct nucleotide in the presence of a mispair. This change in $K_{d(dNTP),app}$ is not accompanied by a change in k_{pol}; values for k_{pol} are the same for both H285D and wild-type. Close examination of available structural data, as well as molecular modeling, has shown that residue 285 is able to make several stabilizing contacts in the fingers domain of the polymerase, and the introduction of a negatively charged side chain could have important effects on the enzyme. It is postulated that the loss of the contact between His285, Lys289, and Ile323 is responsible for the ability of H285D to extend mispairs through disruption of contacts near the C-terminal end of pol β and propagation into the nucleotide binding pocket.

Endogenous DNA damage occurs at a rate of at least 20,000 lesions per cell per day (*2*). These endogenous lesions are repaired by the base excision repair (BER)[1] machinery, and their correct repair is critical for genome stability. A key enzyme in the BER pathway is DNA polymerase beta (pol β), which removes the deoxyribose phosphate group (dRP) and fills in the gap with a nucleotide after the DNA lesion is excised. A relatively error-prone polymerase, pol β inserts an incorrect nucleotide in approximately one out of every 10,000 nucleotide insertions (*3*). Given that BER is responsible for repairing about 20,000 DNA lesions per cell per day, pol β could potentially incorporate incorrect nucleotides on the order of one per cell per day. These errors in DNA repair can be carried through further cell divisions, which can increase genomic instability. Increased genomic instability has been shown to lead to the generation of a mutator phenotype, which in turn can produce a malignant phenotype (*4*).

In BER, damaged DNA bases are recognized and excised by a specific DNA glycosylase, which generates a mutagenic apurinic/apyrimidinic (AP) site (*5*). Next, AP Endonuclease 1 incises the DNA backbone on the 3′ side of the AP site, leaving behind a dRP group (*6*), which is then removed by pol β. Pol β also fills in the single-base gap in the DNA with the correct nucleotide. Lastly, DNA Ligase IIIα seals the nick in the backbone to complete the repair.

Pol β is a 39 kDa protein, which has two catalytic functions: it catalyzes the synthesis of DNA and the removal of dRP groups from DNA (*7*). Pol β does not possess any proofreading exonuclease activity, unlike other eukaryotic polymerases such as pol δ and pol ε (*8*). Pol β functions both in BER and in meiosis (*9*), and additionally, pol β variants have been found in several types of cancerous tissue (*3*). Therefore, studying pol β and its variants can lead to a deeper understanding of the mutational basis of cancer (*10*).

Synthesis of DNA can be abated by the nucleoside analog drug 3′-azido-3′deoxythymidine (AZT). AZT can be incorporated into DNA, but it causes chain termination via the azido group in the 3′ position, which is unable to be extended by the polymerase (*1*). Using an *in vivo* selection, several pol β variants were identified as conferring resistance to AZT to *Escherichia coli* cells (*1*). Three of these variants have already been studied in greater detail *in vitro* (Figure 1a): D246V (*1, 11*), R253M (*1*), and E249K (*12*). The Val246 variant was shown to misincorporate nucleotides through altered DNA positioning in the active site (*11*). The Lys249 variant was shown to be an extender of mispaired primer termini without alteration of the misincorporation fidelity (*12*). The Met253 variant exhibits increased catalytic ef-

* To whom correspondence should be addressed. Tel.: 203-737-2626; fax: 203-785-6309; e-mail: joann.sweasy@yale.edu.
[†] Yale University School of Medicine.
[‡] Center for Medical Sciences, Wadsworth Center, NYS-DOH.
[#] Present address: Division of Maternal and Child Health, School of Public Health, University of California, Berkeley, CA 94720-7360.

[1] Abbreviations: BER - Base Excision Repair; AZT - 3′-Azido-3′-deoxythymidine; pol β - DNA Polymerase Beta; dRP - Deoxyribose phosphate; AP - Apurinic/Apyrimidinic; dNTP - Deoxynucleotide triphosphate; PDB - Protein Data Bank.

10.1021/bi702104y CCC: $40.75
Published on Web 07/11/2008

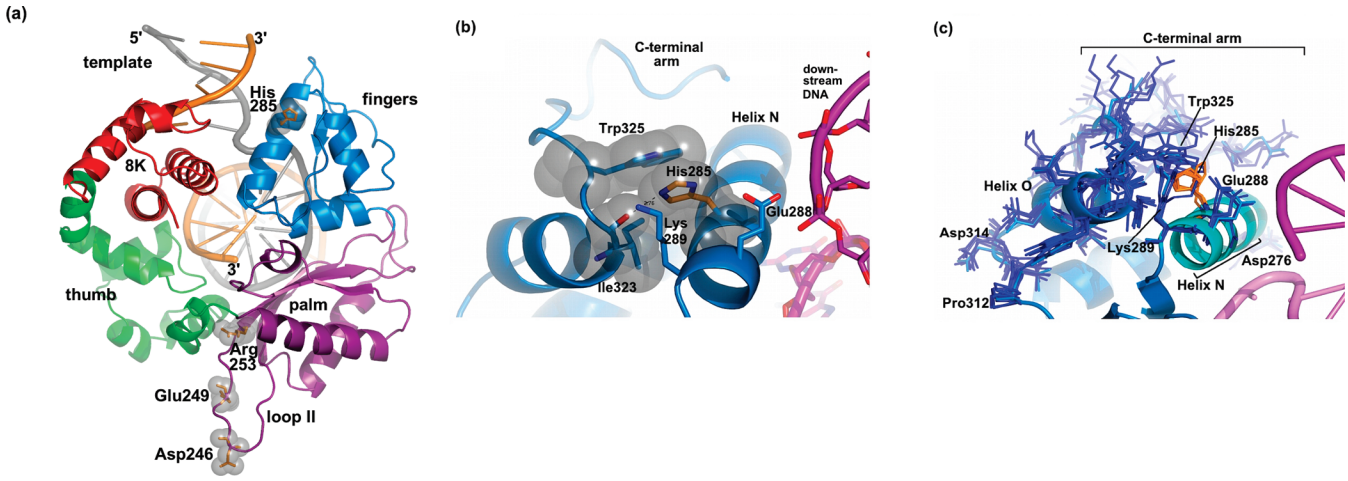

FIGURE 1: (a) Overall structure of pol β complexed with gapped DNA (*29*) in the fully closed conformation colored according to subdomains (8Kd, red; thumb, green; palm, magenta; fingers, blue; 1bpy). Residues Asp246, Glu249, Arg253 and His285, all of which are implicated in AZT resistance (*1*), are shown in orange and highlighted by gray spheres. (b) Close-up view of the pol β fingers domain showing His285 and surrounding residues. His285 (highlighted by orange carbon atoms) is located some 8 Å away from the downstream DNA duplex (deep purple) but points away from the substrate and the polymerase cleft. Instead the imidazole ring of His285 forms hydrogen bond interactions with Ile323 (main chain) and stacks against the aromatic ring of Trp325, thereby stabilizing the flexible C-terminal arm and the fingers domain of pol β. Molecular modeling studies of H285D suggest that the aspartate side chain may form a strong salt bridge with Lys289 at the expense of interacting with C-terminal arm, namely Ile323 and Trp325 in the wild type structure. This in turn could destabilize the fingers domain and further increase the mobility of the C-terminal arm. (c) Comparison of high-resolution DNA cocrystal structures of pol β. The C-terminal arm (residues 323−335) shows a great deal of flexibility while immediately adjacent regions on the surface of the fingers domain, namely Helix N (light blue), Helix O and the long connector (residues 301−315), are far less heterogeneous and much better defined in the crystal structures (*29–32*). The increased flexibility of the C-terminal arm could conceivably have a negative impact on polymerase fidelity and the dNTP binding pocket, which is located directly below Helix N (light blue) next to Asp276. Residue 285, the site of mutation, is located on Helix N and is highlighted in orange. The DNA template is shown in pink and the downstream DNA in purple.

ficiency for incorporation of dTTP while at the same time showing a marked reduction in incorporation of AZT when compared to wild-type (*1*).

The goal of the work presented herein is to examine in detail a fourth AZT-resistant mutant of pol β - the His285 to Asp variant. His285 is located on Helix N in the fingers subdomain of pol β, as shown in Figure 1b. Helix N encompasses residues 275 through 289, which includes several residues that are critical for pol β fidelity. Helix N in pol β contacts the DNA along the minor groove, when the polymerase is in the closed conformation (bound to both DNA and dNTP), and allows for formation of the dNTP binding pocket. Due to altered DNA positioning, the Lys289 to Met variant shows increased misincorporation of dCTP and dGTP opposite template C and G, respectively, and K289 M has been found in colorectal carcinomas (*13*). Alteration of Met282 to Leu causes an increase in the overall stability of pol β, resulting in a reduction in fidelity due to poorer dNTP discrimination at the level of ground-state binding ($K_{d(dNTP)}$) (*14*). Two other important residues reside on Helix N, Asp276 and Arg283 (not shown). Arg283 contacts the minor groove of the DNA substrate on the template side, and its alteration to Ala or Lys results in both deletion and base substitution mutations (*15*). Asp276 when changed to Val allows the polymerase to extend mispaired primer termini without a significant increase in misincorporation events (*16*). His285 is located near the C-terminal end of Helix N and comes in close contact with both Lys289 and Trp325 (Figure 1c). All of these structural clues suggest that mutation of His285 to Asp could indirectly impact the fidelity of pol β. It is presented herein that like the D276V variant, pol β H285D increases the extension frequency of mispaired primer termini without an increase in misincorporation. Through single-turnover kinetics, it is shown that this increase in mispair extension is due to a dramatic increase in nucleotide binding when compared to wild-type pol β.

MATERIALS & METHODS

Protein Expression and Purification. The cDNAs of WT and H285D pol β in the pET28a vector were transformed into the *E. coli* strain BL21 DE3, which has the genotype *F⁻ompT hsdSB*($r_{b-}m_{b-}$)*gal dcm* (DE3). Luria Broth cultures containing 50 μg/mL kanamycin were grown to an OD_{600nm} of ~0.5 and then induced with 1 mM isopropyl β-D-thiogalactopyranoside (IPTG) for 4 h at 30 °C to express the amino-terminal hexahistidine-tagged fusion proteins. The crude proteins were purified using fast protein liquid chromatography. First, using a 5 mL HiTrap Chelating HP column (GE Healthcare) charged with Ni^{2+}, a three step imidazole gradient (25 mM, 300 mM, and 1500 mM) in 40 mM Tris pH 8.0, and 500 mM NaCl was employed. The His-fusion proteins were eluted in the final imidazole step in two or three 2 mL fractions. The fractions were combined, concentrated to <1 mL, and diluted to 10 mL in 50 mM tris pH 8.0, 1 mM EDTA, 10% glycerol, and 100 mM NaCl, which was then run on a 5 mL SP HP column (GE Healthcare) using a linear NaCl gradient from 100 mM to 2000 mM. Purified protein fractions eluted at approximately 1000−1200 mM NaCl in two or three 2 mL fractions. Fractions were combined and concentrated to <1 mL. Glycerol was added to a final concentration of 15%, and 5 μL portions of the final product were flash frozen in a dry ice/ethanol bath and stored at −80 °C. All proteins were purified to >90% homogeneity based on a Coomassie Blue-stained SDS-PAGE gel. Concentrations of pol β were based

Table 1: DNA Substrates[a]

DNA Substrate	
45AG-U22-D22	5′ GCCTCGCAGCCGTCCAACCAAC CAACCTCGATCCAATGCCGTCC 3′ CGGAGCGTCGGCAGGTTGGTTG**A**GTTGGAGCTAGGTTACGGCAGG
CIIX (CIIU + CIID + CIITX; X = A, T, G, or C)	5′ TTGCGACTTATCAACGCCCACA AGTTGTCTTCTCAGTCCT 3′ AACGCTGAATAGTTGCGGGTGT**X**GTCATCAACAGAAGAGTCAGGA (X = A, T, G, or C)
CIIEX (CIIEUX + CIIED + CIIT; X = A, T, G, or C)	5′ TTGCGACTTATCAACGCCCACAT*X* TTGTCTTCTCAGTCCT 3′ AACGCTGAATAGTTGCGGGTGTAG**T**CATCAACAGAAGAGTCAGGA (X = A, T, G, or C)

[a] The 1- and 5-bp gaps are underlined, the templating bases are in boldface, and mispaired termini are in italics.

on ε_{280} = 21,200 M^{-1} cm^{-1} and a molecular mass of 40 kDa for His-tagged pol β.

Circular Dichroism. Both the WT and H285D were examined by circular dichroism in order to determine if the secondary structure content of H285D drastically differed from that of WT. Using 0.2 cm quartz cuvettes in a circular dichroism spectrophotometer (Aviv Model 305SF), the ellipticity of 20 μM enzyme solutions in 10 mM phosphate buffer was measured from 195 to 260 nm at 25 °C.

DNA Substrates. All DNA substrates (Table 1) used in the biochemical assays were constructed from DNA-oligonucleotides that were purchased from The Keck Biotechnology Resource Center at the Yale University School of Medicine. All oligonucleotides were purified by polyacrylamide gel electrophoresis prior to use. The primer and template oligonucleotides were labeled at the 5′ end using T4 polynucleotide kinase (New England Biolabs) and [γ-^{32}P]ATP (Amersham Biosciences). The downstream oliogonucleotide was 5′-labeled with nonradioactive ATP. Kinased oligonucleotides were purified using Microspin columns (Bio-Rad) and annealed at a primer:tempate:downstream ratio of 1:1.2:1.3 in 50 mM Tris and 250 mM NaCl (pH 8.0). The mixtures were heated to 95 °C for 5 min, cooled to 50 °C over 30 min, kept at 50 °C for 20 min, and transferred to ice. The annealing was verified using a 12% native polyacrylamide gel followed by autoradiography.

Pre-Steady-State Kinetic Analysis. Rapid chemical quench kinetics were performed using the Kintek apparatus (*17*). Single-base gapped DNA substrate (45AG-U22-D22, as shown in Table 1) containing a template A opposite the gap was used. Two reaction mixtures (600 nM DNA + 200 nM enzyme and 200 μM dTTP + 20 mM $MgCl_2$) were combined (15 μL each) in the apparatus, rapidly mixed and quenched with 0.5 M EDTA, and combined with 50 μL 90% formamide dye. A time course of reactions from 0.01 to 3.0 s was conducted for both WT and H285D. Final reaction concentrations were 300 nM DNA, 100 nM enzyme, 100 μM dTTP, and 10 mM $MgCl_2$ in reaction buffer (50 mM tris pH 8.0, 20 mM NaCl, 2 mM DTT, and 10% glycerol). Completed reactions were separated using denaturing 20% polyacrylamide gel electrophoresis and visualized and quantitated using a Storm 860 phosphorimager with ImageQuant software. Kinetic data were plotted and fit using Kaleidagraph software (Synergy software) to the biphasic burst equation:

$$[\text{product}] = A(1 - e^{k_{obs}t} + k_{ss}t) \quad (1)$$

where A is the amplitude, k_{obs} is the observed rate constant of the exponential phase, and k_{ss} is the rate constant for the linear (or steady-state) phase (*18*).

Gel Mobility Shift Assay. In order to assess the binding of wild-type and H285D pol β to DNA, CIIEC (5bp-gap) DNA (Table 1) was used with both wild-type and H285D in gel mobility shift assays. DNA (0.1 nM) was incubated with varying amounts of pol β (0.015−1000 nM) in binding buffer (10 mM Tris-HCl pH 7.6, 6 mM $MgCl_2$, 100 mM NaCl, 10% glycerol, 0.1% IGEPAL) for 15 min at room temperature. A 6% Native PAGE gel, prerun at 150 V for 1 h at 4 °C, was loaded with samples of the reactions while the current was running at 300 V. Once the samples had left the wells, the gel was run for approximately three hours at 150 V at 4 °C, dried, and exposed in a phosphorimager cassette for 72−120 h. The data were gathered and quantitated by phosphorimager. Plotting percent bound DNA vs the log of [DNA] in nM and fitting the data to the following equation:

$$Y = \frac{m[\text{protein}]}{[\text{protein}] + K_{D(DNA)}} + b \quad (2)$$

where Y is the amount of bound protein, m is a scaling factor, and b is the apparent minimum Y value, yielded the apparent $K_{D(DNA)}$ for each enzyme on a 5-bp gapped DNA substrate (*18*).

Primer Extension Assays. Primer extension assays were conducted using all four CIIX 5-base-pair gaped DNA substrates (Table 1). Two reaction mixtures were prepared in reaction buffer (50 mM tris pH 8.0, 20 mM NaCl, 2 mM dithiothreitol, and 10% glycerol). The first contained pol β (1.5 μM) and DNA (100nM), and the second consisted of 100 μM of each dNTP and 20 mM $MgCl_2$. 20 μL of each mix were incubated for 1 min at 37 °C and then combined together (final concentrations in reaction: 750 nM pol β, 50 nM DNA, 50 μM dNTPs, and 10 mM $MgCl_2$) and incubated for an additional 5 min at 37 °C. After 5 min, the reactions were quenched by the addition of 50 μL of 1:1 90% formamide dye:0.5 M EDTA and placed immediately on ice. The completed reaction mixtures were resolved on a 20% denaturing polyacrylamide gel and the products were visualized using a phosphor screen and imager. Two types of primer extension assays were performed. The "Missing Base Primer Extension" used three of the four dNTPs, while the "One at a Time Primer Extension" used only one of the four dNTPs. The exact dNTPs used in each reaction are noted in the figures.

Single Turnover Extension Assays. In order to examine the ability of H285D to extend mispaired primer termini,

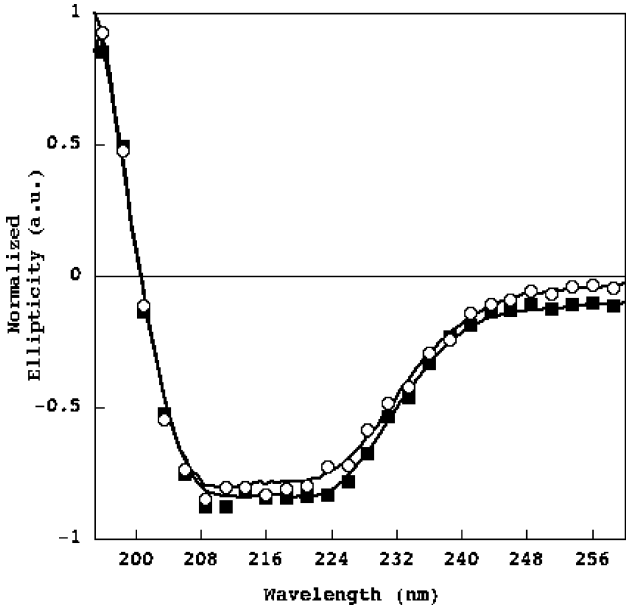

FIGURE 2: The Asp285 mutation does not alter the overall structure of pol β. Circular dichroism spectra of 20 μM wild-type (○) and H285D (■) pol β in 10 mM phosphate buffer at 25 °C collected in 0.2 cm quartz cuvettes from 195 to 260 nm (a.u. = absorbance units).

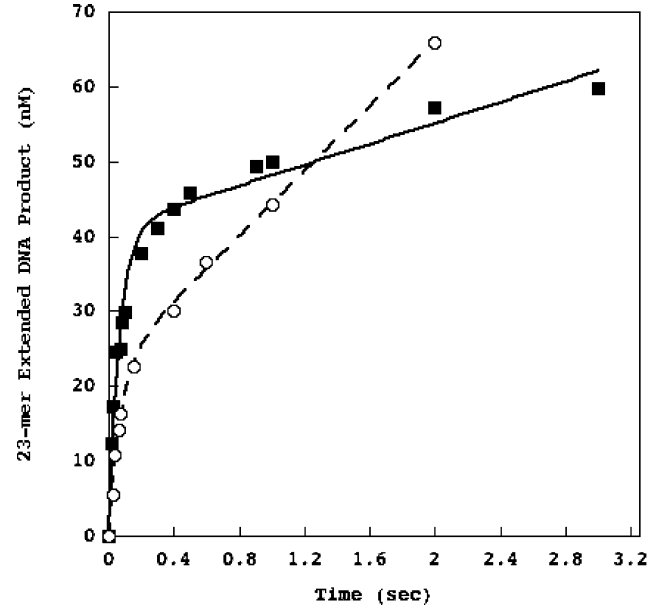

FIGURE 3: The H285D mutant exhibits pre-steady-state kinetics similar to wild-type. Pre-steady-state burst kinetics were performed as described in Materials and Methods using 1 bp-gapped DNA (45AG-U22-D22; Table 1). For both wild-type and H285D, 100 μM dTTP, 10 mM $MgCl_2$, 300 nM DNA, and 100 nM pol β were reacted in a time course form 0.01 to 3.0 s. DNA products, resolved on a sequencing gel, were quantified and plotted vs time to generate the burst plots for wild-type (○; k_{obs} = 14 s^{-1}, k_{ss} = 0.97 s^{-1}, amplitude = 23) and H285D (■; k_{obs} = 16 s^{-1}, k_{ss} = 0.18 s^{-1}, amplitude = 41) pol β.

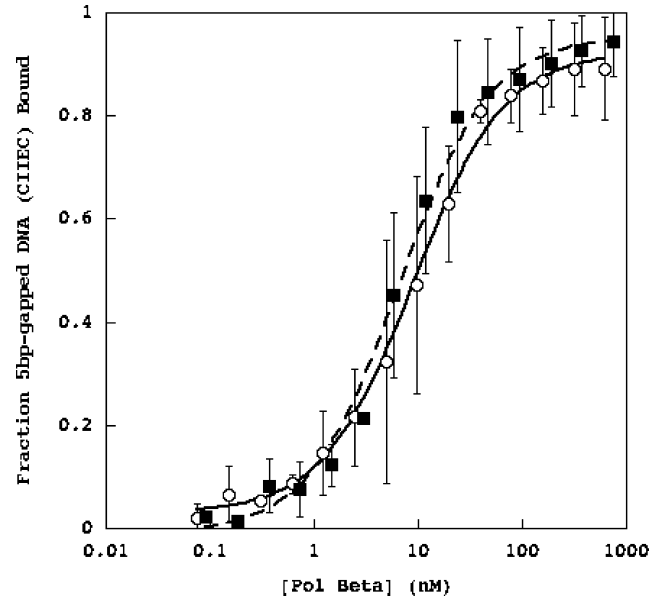

FIGURE 4: The H285D mutant has similar binding affinity for 5-bp gapped DNA as the wild-type. DNA (0.1nM) was incubated with varying amounts of pol β (0.015−1000 nM) in binding buffer for 15 min at room temperature. Sigmoidal plots of fraction of DNA bound vs the log of protein concentration show no difference between wild-type (■) and H285D (○) pol β: $K_{D(DNA)} = 6.7 \pm 0.8$ and 9.2 ± 0.7 nM, respectively.

single turnover extension assays were performed using the CIIEX series of 5 bp gapped DNA substrates, as shown in Table 1. Single turnover assays allow for the determination of the apparent binding constant for dATP (K_d) and the maximum rate of polymerization (k_{pol}). For mispaired termini, CIIEX substrates where X is A, T, or G, time courses from 20 s to 60 min were performed manually at 37 °C using dATP concentrations between 1.0 μM and 3.0 mM. Mixtures of 50 nM DNA and 1.5 μM (WT) or 4 μM (H285D) in reaction buffer (see above) were incubated at 37 °C for 5 min, and then, dATP/$MgCl_2$ mixtures in reaction buffer were added to produce the final reaction concentrations (750 nM and 2 μM for WT and H285D, respectively). Aliquots of the reactions (20 μL) were quenched at various time points with 25 μL of 1:1 90% formamide dye:0.5 M EDTA and placed immediately on ice. For the 5bp DNA substrate with a correctly paired terminus, CIIEC, reactions were conducted using the Kintek rapid quench flow apparatus (*17*) as explained above for pre-steady-state assays. Final enzyme and DNA concentrations were the same as for mispaired DNA substrates, and the concentrations of dATP used ranged from 1 to 100 μM. Completed reaction mixtures were separated using denaturing 20% polyacrylamide gel electrophoresis, and products were quantitated via phosphorimager, as explained in greater detail above. The single turnover kinetic data were fit to a single exponential equation using the Kaleidagraph software (Synergy Software):

$$[\text{product}] = A(1 - e^{k_{obs}t}) \quad (3)$$

where A is the amplitude, k_{obs} is the observed rate constant and t is the time (*19*). A secondary kinetic plot was constructed by plotting the observed rate constant (k_{obs}) vs [dATP], which was then fit to the hyperbolic equation:

$$k_{obs} = \frac{k_{pol}[\text{dATP}]}{K_d + [\text{dATP}]} \quad (4)$$

where $k_{pol}$is the maximum rate of polymerization and K_d is the apparent equilibrium dissociation constant of dATP (*19*).

Molecular Modeling. The programs PyMol 0.99 (*20*) and Coot 0.33 (*21*) were used to inspect and compare several DNA cocrystal structures of wild-type pol β. His285 was mutated to Asp with PyMol and potential spatial overlaps

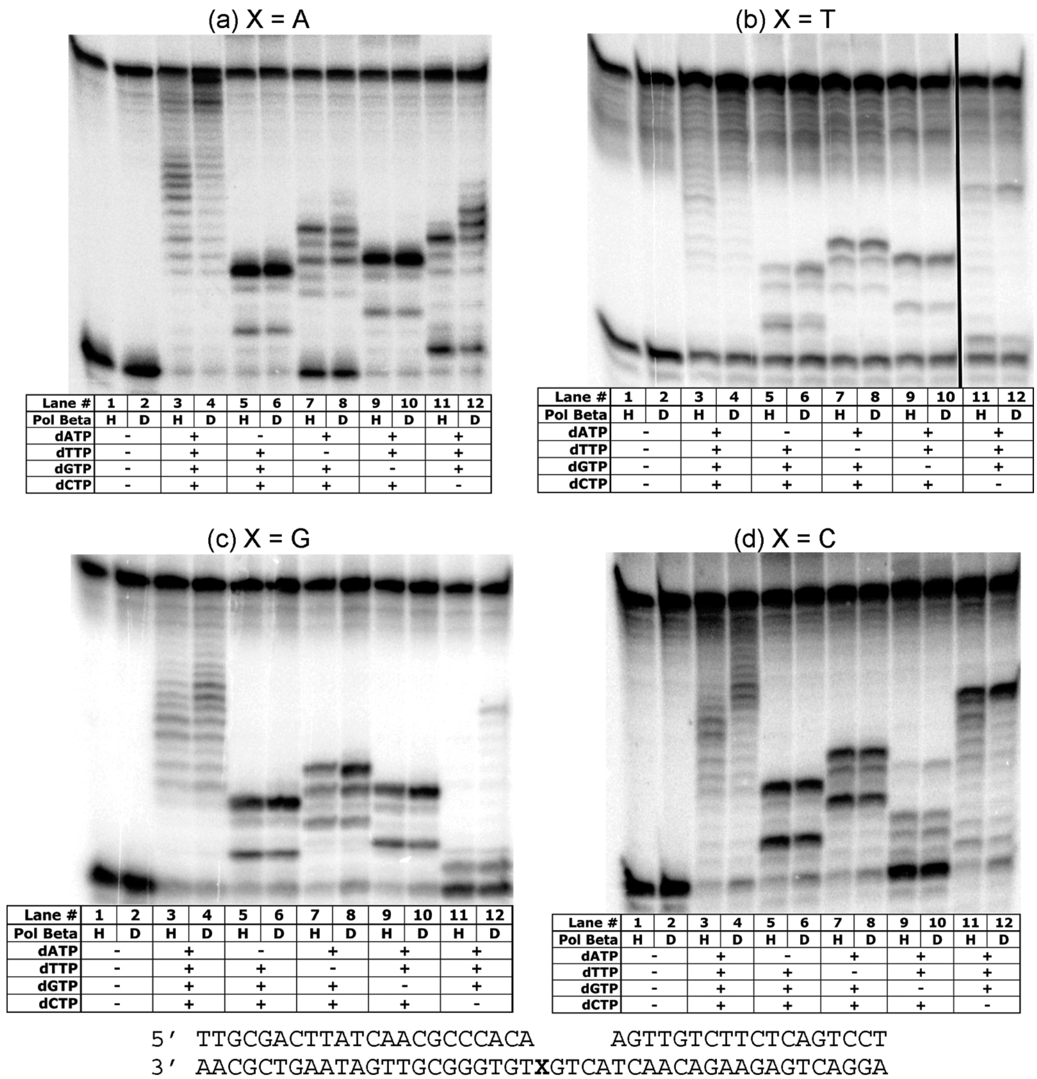

FIGURE 5: Pol β H285D exhibits a mild mutator phenotype in missing base incorporation assays. Phosphorimager scans of 20% denaturing PAGE gels for missing base primer extension assays with (a) CIIA, (b) CIIT, (c) CIIG, and (d) CIIC 5-bp gapped DNA substrates. In each panel, lanes 1, 3, 5, 7, 9, and 11 are reactions with wild-type pol β (H) and lanes 2, 4, 6, 8, 10, and 12 are reactions with pol β H285D (D). Reactions were conducted with various dNTPs as indicated.

with neighboring residues were inspected. The resulting H285D model was then subjected to energy minimization and fully solvated equilibration using the program NAMD 2.0 (*22*).

RESULTS

Pol β H285D Retains a Similar Global Structure as Wild-Type. Circular dichroism was employed in order to verify the secondary structure content and the overall fold of the H285D mutant. The spectra of both WT and H285D have the same shape (Figure 2), indicating that the secondary structure content of the two proteins are essentially the same. This suggests that both H285D and WT have the same fold and that the overall structure is presumably not altered by replacing His285 with Asp.

H285D Exhibits Biphasic Burst Kinetics. Using a 3-fold excess of 1bp-gapped substrate, WT pol β shows biphasic burst kinetics (Figure 3) with an observed rate constant (k_{obs}) of 14 $\pm$ 2 s^{-1}, which is in close agreement with previously reported values (*23*). The pre-steady-state burst plot for the H285D variant of pol β also exhibits biphasic shape with a similar k_{obs} of 16 $\pm$ 1 s^{-1} (Figure 3). This suggests that both of these enzymes are following the same mechanism, wherein the chemistry step of the addition of nucleotide is rapid (exponential phase) followed by a much slower product release step (linear phase), which in both cases is the rate limiting step (*24*). We realize that our results provide no information about the rate of conformational changes that could be altered in the variant. However, the steady-state rate, indicated by the linear portion of the curve, for H285D is much slower than that of WT (k_{ss} = 0.18 and 0.97 s^{-1}, respectively); thus, it is likely that H285D releases the extended DNA product more slowly than the WT pol β. The amplitude of the burst curve for the H285D variant is somewhat higher than that of wild-type (amplitude = 41 and 23, respectively). The amplitude reflects the number of active sites of enzyme in the preparation. In two separate protein preparations, we have observed this difference.

H285D Has Similar Affinity for DNA as Wild-Type Pol β. The interaction of these proteins with a 5-bp gapped DNA substrate was examined using the CIIEC substrate (Table 1). The $K_{D(DNA)}$ values for the 5-bp gapped DNA substrate

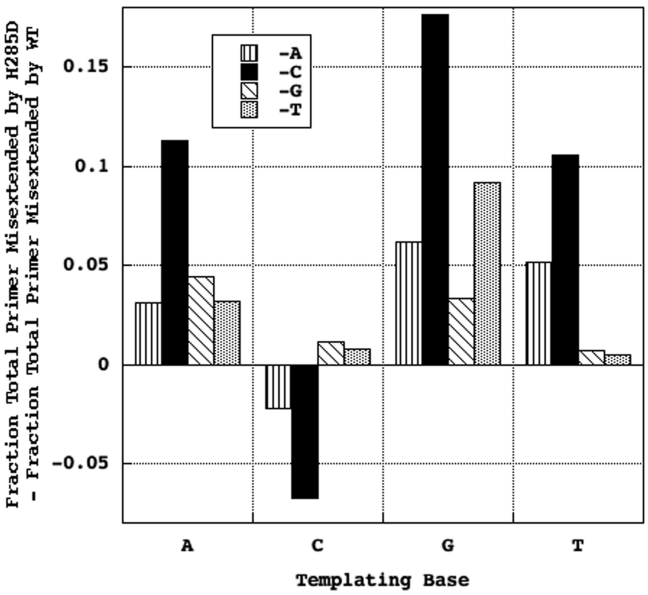

FIGURE 6: Pol β H285D misextends DNA substrates more than wild-type. Bands from the missing base primer extension gel (Figure 5) were quantified and the fraction of total primer misextended by pol β was calculated for both wild-type and H285D pol β under each set of reaction conditions. The difference between misextension by H285D and misextension by wild-type pol β for each DNA substrate is shown. Pol β H285D misextends DNA substrates more than wild-type by roughly 10% when dCTP is absent from the polymerase reactions.

were similar for wild-type and H285D pol β (6.7 $\pm$ 0.8 and 9.2 $\pm$ 0.7 nM, respectively, Figure 4).

Pol β H285D Is a Subtle Mutator Polymerase. To examine the ability of H285D to misincorporate nucleotides and extend mispaired bases, missing base primer extension assays were performed using the four different CIIX 5-bp gapped DNA substrates as described in Materials & Methods. In each case, H285D is able to completely fill in the gap and continue the synthesis past the gap when given all four dNTPs in the same manner as WT (Figure 5, Lanes 3 and 4). In separate experiments with each of the four CIIX DNA substrates, H285D showed similar reaction patterns as those of WT pol β, indicating that both enzymes have the ability to misincorporate and misextend nucleotides. However, H285D did show a slightly increased ability to extend farther than WT (approximately 10%, Figure 6) in reactions where dCTP was absent (Figure 5, Lanes 11 and 12). This suggests that H285D could be capable of extending mispaired termini more efficiently than WT, especially opposite a template G.

Pol β H285D Does Not Misincorporate Nucleotides More than Wild-Type Pol β. One at a time primer extension assays, using the same 5-bp gapped DNA substrates as above, were performed as described in Materials & Methods in order to determine if the Asp285 variant of pol β misincorporates nucleotides more efficiently than WT does. As with the missing base primer extension assays described above, the control reactions with all four dNTPs and no dNTPs looked exactly the same for all four substrates with both WT and H285D (Figure 7, Lanes 3 and 4). In four separate experiments with each of the CIIX DNA substrates, both H285D and WT pol β show the same pattern of primer extension (Figure 7). This suggests that H285D is not misincorporating nucleotides at an increased frequency compared to wild-type. This would also imply that the slight mutator activity seen in the missing base primer extension assay (Figure 5) is due to an increased ability to extend mispaired primer termini and not due an increase in misincorporation of nucleotides.

Pol β H285D Extends Mispaired Termini Opposite Template G. Single turnover mispair extension assays were employed to more fully examine the ability of H285D and wild-type pol β to extend mispaired primer termini opposite template G. Four different substrates were used to examine the three possible mispairs with template G (A:G, T:G, and G:G) as well as the correctly paired primer terminus (C:G). The assays utilizing the DNA substrate with the correctly paired primer terminus (CIIEC) were conducted using the rapid quench flow apparatus as described in Materials & Methods. The maximum rate of polymerization for both WT and H285D were similar (Table 2). Both the wild-type enzyme and the H285D variant were able to extend the primer by one nucleotide when the correct nucleotide was present (dATP). However, the apparent $K_{d(dATP)}$ for H285D is 42-fold lower than that of wild-type (Table 2). This indicates that H285D binds to the incoming nucleotide much more tightly than does the wild-type pol β. This is also the case with the extension of all three of the DNA substrates with mispaired primer termini (Table 2). An example of the results of extension of a T:G mispaired primer terminus by H285D is shown in Figure 8. In each case, the rate of polymerization is unaffected by the His to Asp alteration. Additionally, with every DNA substrate the $K_{d(dATP),app}$ for H285D is at least an order of magnitude lower than that of the corresponding wild-type pol β. These data show that even when the Asp285 variant polymerase is given an unfavorable substrate (i.e., one with a mispaired primer terminus) the polymerase binds to the incoming next correct nucleotide (dATP) much more tightly than does the wild-type polymerase. This increased binding by pol β H285D leads to much higher polymerization efficiencies when compared to the wild-type enzyme (k_{pol}/K_d; Table 2).

DISCUSSION

The Asp285 variant of pol β is a mutator polymerase, due to the enzyme's ability to extend mispaired primer termini. Mispair extension is increased in the mutant due to its tighter binding of nucleotide substrate. It is proposed that this increased ability to bind to nucleotide substrate is due to the rearranging of interactions among amino acid residues surrounding His285. The AZT resistance of H285D and its ability to extend mispaired primer termini parallel the E249K pol β mutant, despite the fact that neither residue is near the active site and that the two residues are located far from one another. This supports our hypothesis that residues that are far removed from the active site of DNA polymerase β play important roles in maintaining polymerase fidelity.

Pol β H285D Is a Mutator Polymerase. Primer extension assays in which both the mutant and wild-type were used to fill in a five base-pair gap indicate that H285D has a fidelity similar to the wild-type polymerase. There does exist, however, a notable exception. In gap-filling assays with three out of four nucleotides with dCTP missing, H285D exhibits an increase in extended DNA products when compared to the wild-type enzyme (Figure 5). This indicates that H285D is more capable of either misincorporating and/or extending mispaired primer termini opposite template G than wild-type.

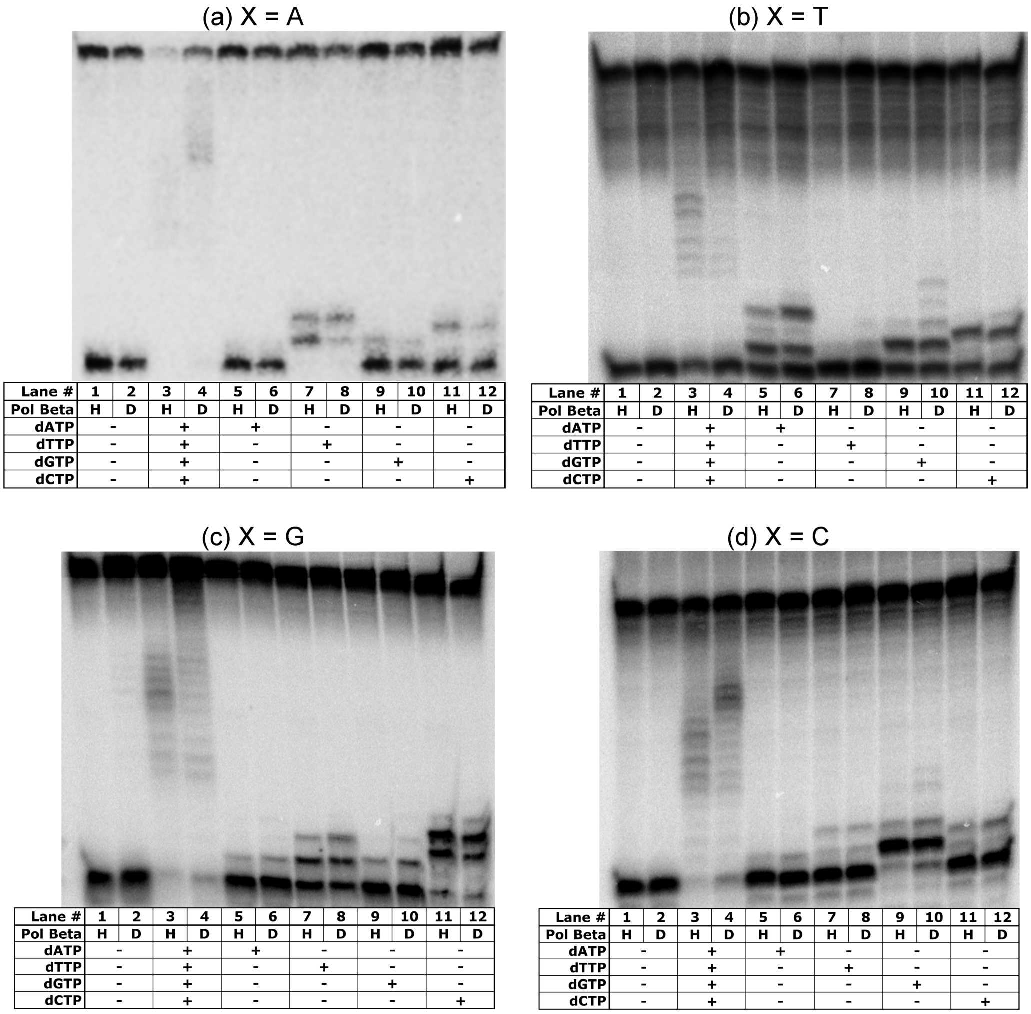


```
5’ TTGCGACTTATCAACGCCCACA      AGTTGTCTTCTCAGTCCT
3’ AACGCTGAATAGTTGCGGGTGTXGTCATCAACAGAAGAGTCAGGA
```

FIGURE 7: Pol β H285D does not misincorporate nucleotides more than wild-type pol β. Phosphorimager scans of 20% denaturing PAGE gels for missing base primer extension assays with (a) CIIA, (b) CIIT, (c) CIIG, and (d) CIIC 5-bp gapped DNA substrates. In each panel, lanes 1, 3, 5, 7, 9, and 11 are reactions with wild-type pol β (H) and lanes 2, 4, 6, 8, 10, and 12 are reactions with pol β H285D (D). Reactions were conducted with various dNTPs as indicated.

Table 2: Pol β H285D Extends Mispaired Primer Termini[a]

DNA substrate	primer terminus[b]	pol β	k_{pol} (s^{-1})	$K_{d(dATP)}$[c] (μM)	k_{pol}/K_d (M^{-1} s^{-1})
CIIEC	C:G	WT	2.98 ± 0.05	183 ± 5	16300
		H285D	2.5 ± 0.2	4.4 ± 0.9	5700000
CIIET	T:G	WT	0.105 ± 0.004	130 ± 20	810
		H285D	0.17 ± 0.01	10 ± 1	17000
CIIEA	A:G	WT	0.060 ± 0.004	540 ± 90	110
		H285D	0.0748 ± 0.0006	27.8 ± 0.9	2690
CIIEG	G:G	WT	<0.0054[d]	>3000[d]	<2[e]
		H285D	0.0078 ± 0.0004	610 ± 70	13

[a] Kinetic data gathered from single turnover mispair extension experiments are shown for four different DNA substrates for both wild-type and the Asp285 variant. $K_{d(dATP)}$ is the equilibrium dissociation constant for dATP, k_{pol} is the maximum rate of polymerization, and k_{pol}/K_d is a measure of the enzyme's catalytic efficiency. The $K_{d(dATP)}$ value for wild-type on the CIIEG substrate is estimated due to the fact that wild-type did not completely extend this mispair, even at high concentrations of dATP. [b] Base on the template strand is underlined. [c] Apparent $K_{d(dATP)}$. [d] Estimate. [e] Maximum efficiency based on estimated data.

In order to examine the misincorporating ability of the mutant, the same 5-bp gapped DNA substrate was used in experiments containing only one dNTP. In each case (four different DNA substrates with each possible dNTP), H285D showed the same profile as wild-type (Figure 7), which indicates that the mutant is not misincorporating nucleotides more than wild-type pol β. Thus, H285D is extending mispaired primer termini opposite template G.

Mispaired Guanine Primer Termini Are Extended More Readily by H285D. Four different 5-bp gapped DNA substrates (one with each possible primer terminus opposite template G, Table 1) were used in single-turnover mispair extension experiments, which are described in detail in Materials & Methods. In every case, H285D displayed a similar rate constant for polymerization (k_{pol}) as the wild-type enzyme, which only changed from 0.6 to 1.2-fold over WT, indicating that the geometry of the active site and the coordination of the magnesium ions by active site residues is presumably unaffected by the His285 to Asp mutation.

However, in contrast to the lack of effect on k_{pol}, the apparent $K_{d(dATP)}$ values are drastically affected by the mutation. On each one of the four DNA substrates that were examined in the single-turnover experiments, the $K_{d(dATP),app}$ values for the mutant were reduced up to 42 fold compared to wild-type, indicating that H285D binds nucleotide much

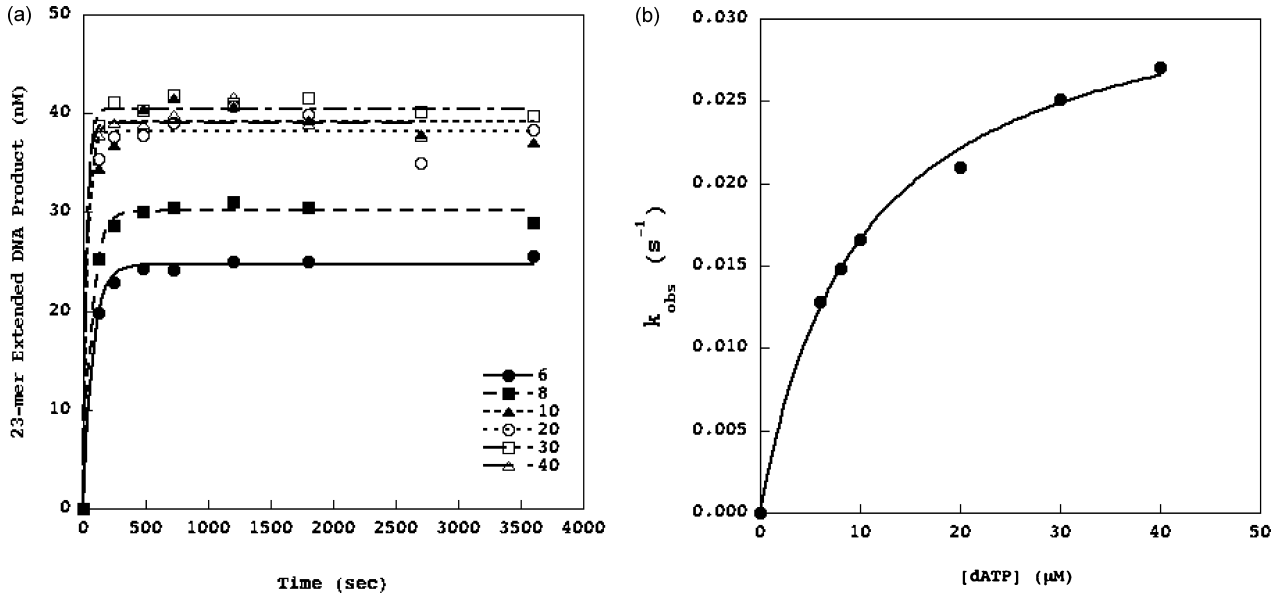

FIGURE 8: Pol β H285D efficiently extends a T:G mispaired primer terminus in 5-bp gapped DNA. Correct incorporation of dATP opposite template T adjacent to a T:G mispaired primer terminus (CIIET). (a) The plot of nM of 23-mer extended DNA product formed vs time for H285D at six different concentrations of dATP (6, 8, 10, 20, 30, and 40 μM dATP) fit to a single exponential equation to obtain the observed rate constant (k_{obs}) for each concentration of dATP. (b) The secondary kinetic plot of k_{obs} vs [dATP] for H285D fit to a hyperbolic equation to obtain k_{pol} and apparent K_d for dATP (0.17 s^{-1} and 10 μM, respectively).

more tightly than the wild-type polymerase, even in the presence of an incorrectly paired primer terminus. The trend in the both the k_{pol} and $K_{d(dATP),app}$ values for both enzymes is what would be expected based on the geometry of the mispaired termini (*25*). The correct terminus (C:G) is extended the fastest of the four with the tightest binding to the next correct incoming nucleotide (dATP). The T:G mispair, being the least geometrically distorted of the three mispaired termini, has the largest k_{pol} and the smallest $K_{d(dATP),app}$, which means that it is extended the fastest and the incoming nucleotide is bound the tightest of the three mispaired termini. The two purine:purine mispaired termini (A:G and G:G) exhibit far slower polymerization rates (k_{pol} = 0.0748 and 0.0078 s^{-1} for H285D, respectively) and greatly increased dissociation constants for dATP ($K_{d(dATP),app}$ = 27.8 and 610 μM for H285D, respectively) when compared to the pyrimidine-purine pairs. However, in both purine:purine cases the difference in K_d between H285D and the wild-type is increased over the pyrimidine:purine pairs.

Wild-Type Pol β Does Not Extend G:G Mispaired Termini. The G:G primer terminus is a special case in this study. In the single-turnover mispair extension experiments, accurate values for k_{pol} and $K_{d(dATP),app}$ are only achieved when the extended primer product reaches saturation at or above 80%. The G:G primer terminus is extended by the H285D mutant polymerase well enough to calculate accurate k_{pol} and $K_{d(dATP),app}$ values (Table 2); however, the wild-type pol β was able to produce a maximum of less than 50% extended primer product even with dATP concentrations as high as 3 mM (data not shown).

Increased dATP Binding May Be Due to Changes in the Nucleotide Binding Pocket. Upon binding of dNTP substrate, pol β undergoes a conformational change from an open form to a closed form (*26, 27*). Helix N, located on the fingers domain of pol β, moves a distance of about 8.7 Å, based on the location of Lys289-Cα at the C-terminal ends of this helix in the binary and ternary complex, respectively (see PDB; 1bpx and 1bpy). The conformational change forms the catalytically relevant nucleotide binding pocket around the dNTP. Several Helix N mutants of pol β have been isolated and characterized previously (*13–16*). Two of these mutants, D276V and M282L, have been shown to bind to the incoming nucleotide more tightly than wild-type. Interestingly, the side chains of both Asp276 and Met282 are not located in the vicinity of the DNA template. Similarly, the imidazole group of His285 is some 8.0 Å away from the DNA template and, therefore, does not directly contact the substrate. Surprisingly though, H285D binds the incoming nucleotide more tightly than wild-type pol β.

The nucleotide binding pocket of pol β consists of residues 271, 272, 276, 279 on pol β and the templating base and the primer terminus on the DNA and is located at the end of Helix N, close to the active site. The D276V and M282L mutants exhibit increased nucleotide binding compared to wild-type pol β, which suggests that mutations in Helix N do somehow affect the nucleotide binding pocket. By careful examination of the nearest neighbors of His285 in the fully closed ternary complex in which the nucleotide binding pocket is correctly formed, one can visualize how the mutation of His285 to Asp could affect the nucleotide binding pocket. Examination of the residues surrounding His285 in the ternary complex yields several interesting contacts (Figure 1b). In addition to being in close proximity to Lys289, the imidazole nitrogen forms a hydrogen bond with the backbone carbonyl oxygen of Ile323. Modeling and energy minimization of Asp in this position indicates that the distance between Lys289 and Asp285 may be reduced by formation of a salt bridge and the distance between Ile323 and both Lys289 and Asp285 increases significantly. The interactions of the nitrogen atoms of Lys289 and His285 with the carbonyl oxygen of Ile323 are presumably important for keeping the C-terminal residues (320−335) of pol β anchored in place.

Furthermore, in wild-type pol β the imidazole ring of His285 forms a partial stacking interaction with the indole

ring of Trp325 (Figure 1b). In addition to the hydrogen bond with Ile323, this stacking interaction further stabilizes the C-terminal end of pol β. In H285D, however, the carboxylate group of Asp285 moves away from the 323/325 moiety by adopting the most frequently used Asp rotamer and forming a salt bridge with Lys298. This could possibly lead to a destabilization of the C-terminal arm in the mutant. Comparison of well-refined high-resolution structures of pol β and analysis of temperature factors in this region suggests that the C-terminal arm of pol β is flexible (Figure 1c). Altering His285 to Asp and loss of the interaction between residues 285, 323 and 325 perhaps allow this arm to adopt conformations which would alter the position of the C-terminal end near the nucleotide binding pocket. These alterations around the C-terminal residues could affect the shape of the NTP binding pocket and, thus, could possibly have an effect on nucleotide binding.

AZT Resistance and E249K Pol β. Strikingly, another AZT-resistant mutant has similar fidelity characteristics as H285D. Both mutants are mispair extenders and both are AZT resistant. Interestingly, Glu249 and His285 are on opposite sides of the enzyme and both are far removed from the active site. Glu249 is located on the solvent-exposed Loop II in the palm domain (*1, 12, 28*). It has been postulated that Loop II of pol β acts as a type of fulcrum, positioning the template strand of the DNA properly in the active site. Alterations of this loop lead to mutants with varying degrees of activity and fidelity. This, however, is not the mechanism in play with H285D. Instead, H285D exerts its AZT resistance through the binding of nucleotide substrate. We believe that the tighter binding of nucleotide by the Asp285 variant of pol β allows the enzyme to be more selective in its choice of nucleotides when the primer-terminus is correctly paired. This tighter binding gives the enzyme enough time to perform the S_N2 substitution reaction at the 3′-OH of the primer strand. AZT, which possesses an unfavorable conformation in the nucleotide binding pocket, becomes excluded due to the mutant's increased binding affinity.

On the contrary, this tight nucleotide binding that affords the variant's AZT resistance also allows for a greatly increased ability to extend mispaired primer termini. Ultimately, this is an undesirable property in that it allows mutations in the DNA to become locked in place, which can lead to further genomic instability. It is possible that pol β evolved to have a binding pocket with a lower affinity for nucleotide, in order to avoid this issue of mispair extension. By allowing the enzyme to sample the many choices of nucleotide available, through weaker nucleotide binding, pol β is able to discern whether or not the primer terminus should be extended. This leaves the opportunity for the error in DNA synthesis to be corrected.

ACKNOWLEDGMENT

We thank Dr. Shibani Dalal for help and suggestions throughout this study. We also thank members of the Sweasy laboratory. This research was supported by HRI New Investigator Funds (J.J.) and NIH grant CA80830 (J.B.S.).

REFERENCES

1. Kosa, J. L., and Sweasy, J. B. (1999) 3′-Azido-3′-deoxythymidine-resistant mutants of DNA polymerase beta identified by in vivo selection. *J. Biol. Chem. 274*, 3851–3858.
2. Lindhal, T. (1993) Instability and decay of the primary structure of DNA. *Nature 362*, 709–715.
3. Starcevic, D., Dalal, S., and Sweasy, J. B. (2004) Is There a Link Between DNA Polymerase b and Cancer? *Cell Cycle 3*, 998–1001.
4. Venkatesan, R. N., Bielas, J. H., and Loeb, L. A. (2006) Generation of Mutator Mutants during Carcinogenesis. *DNA Repair 5*, 294–302.
5. Dianov, G. L., Sleeth, K. M., Dianova, I. I., and Allinson, S. L. (2003) Repair of abasic sites in DNA. *Mutat. Res. 531*, 157–163.
6. Wong, D., DeMott, M. S., and Demple, B. (2003) Modulation of the 3′→5′-exonuclease activity of human apurinic endonuclease (Ape1) by its 5′-incised Abasic DNA product. *J. Biol. Chem. 278*, 36242–36249.
7. Prasad, R., Beard, W. A., Strauss, P. R., and Wilson, S. H. (1998) Human DNA polymerase beta deoxyribose phosphate lyase. Substrate specificity and catalytic mechanism. *J. Biol. Chem. 273*, 15263–15270.
8. Pavlov, Y. I., Maki, S., Maki, H., and Kunkel, T. A. (2004) Evidence for interplay among yeast replicative DNA polymerases alpha, delta and epsilon from studies of exonuclease and polymerase active site mutations. *BMC Biol. 2,* 11.
9. Plug, A. W., Clairmont, C. A., Sapi, E., Ashley, T., and Sweasy, J. B. (1997) Evidence for a role for DNA polymerase beta in mammalian meiosis. *Proc. Natl. Acad. Sci. U. S. A. 94*, 1327–1331.
10. Loeb, L. A., Loeb, K. R., and Anderson, J. P. (2003) Multiple mutations and cancer. *Proc. Natl. Acad. Sci. U. S. A. 100*, 776–781.
11. Dalal, S., Kosa, J. L., and Sweasy, J. B. (2004) The D246V mutant of DNA polymerase beta misincorporates nucleotides: evidence for a role for the flexible loop in DNA positioning within the active site. *J. Biol. Chem. 279*, 577–584.
12. Kosa, J. L., and Sweasy, J. B. (1999) The E249K mutator mutant of DNA polymerase beta extends mispaired termini. *J. Biol. Chem. 274*, 35866–35872.
13. Lang, T., Maitra, M., Starcevic, D., Li, S. X., and Sweasy, J. B. (2004) A DNA polymerase beta mutant from colon cancer cells induces mutations. *Proc. Natl. Acad. Sci. U. S. A. 101*, 6074–6079.
14. Shah, A. M., Conn, D. A., Li, S. X., Capaldi, A., Jager, J., and Sweasy, J. B. (2001) A DNA polymerase beta mutator mutant with reduced nucleotide discrimination and increased protein stability. *Biochemistry 40*, 11372–11381.
15. Osheroff, W. P., Beard, W. A., Yin, S., Wilson, S. H., and Kunkel, T. A. (2000) Minor groove interactions at the DNA polymerase beta active site modulate single-base deletion error rates. *J. Biol. Chem. 275*, 28033–28038.
16. Vande Berg, B. J., Beard, W. A., and Wilson, S. H. (2001) DNA structure and aspartate 276 influence nucleotide binding to human DNA polymerase beta. Implication for the identity of the rate-limiting conformational change. *J. Biol. Chem. 276*, 3408–3416.
17. Johnson, K. A. (1993) Conformational coupling in DNA polymerase fidelity. *Annu. Rev. Biochem. 62*, 685–713.
18. Dalal, S., Chikova, A., Jaeger, J., and Sweasy, J. B. (2008) The Leu22Pro tumor-associated variant of DNA polymerase beta is dRP lyase deficient. *Nucleic Acids Res. 36*, 411–422.
19. Li, S. X., Vaccaro, J. A., and Sweasy, J. B. (1999) Involvement of phenylalanine 272 of DNA polymerase beta in discriminating between correct and incorrect deoxynucleoside triphosphates. *Biochemistry 38*, 4800–4808.
20. DeLano, W. L. (2006) *The PyMOL Molecular Graphics System*, DeLano Scientific LLC, San Carlos, CA, USA. http://www.pymol.org.
21. Emsley, P., and Cowtan, K. (2004) Coot: Model-Building Tools for Molecular Graphics. *Acta Crystallogr. Sect. D 60*, 2126–2132.
22. Kal, L., Skeel, R., Bhandarkar, M., Brunner, R., Gursoy, A., and Krawetz, A. (1999) NAMD2: Greater scalability for parallel molecular dynamics. *J. Comp. Phys. 151*, 283–312.
23. Werneburg, B. G., Ahn, J., Zhong, X., Hondal, R. J., Kraynov, V. S., and Tsai, M. D. (1996) DNA polymerase beta: pre-steady-state kinetic analysis and roles of arginine-283 in catalysis and fidelity. *Biochemistry 35*, 7041–7050.
24. Kati, W. M., Johnson, K. A., Jerva, L. F., and Anderson, K. S. (1992) Mechanism and fidelity of HIV reverse transcriptase. *J. Biol. Chem. 267*, 25988–25997.
25. Yang, L., Beard, W., Wilson, S., Roux, B., Broyde, S., and Schlick, T. (2002) Local deformations revealed by dynamics simulations of DNA polymerase Beta with DNA mismatches at the primer terminus. *J. Mol. Biol. 321*, 459–478.

26. Bakhtina, M., Lee, S., Wang, Y., Dunlap, C., Lamarche, B., and Tsai, M. D. (2005) Use of viscogens, dNTPalphaS, and rhodium(III) as probes in stopped-flow experiments to obtain new evidence for the mechanism of catalysis by DNA polymerase beta. *Biochemistry 44*, 5177–5187.
27. Kim, S. J., Beard, W. A., Harvey, J., Shock, D. D., Knutson, J. R., and Wilson, S. H. (2003) Rapid segmental and subdomain motions of DNA polymerase beta. *J. Biol. Chem. 278*, 5072–5081.
28. Lin, G. C., Jaeger, J., and Sweasy, J. B. (2007) Loop II of DNA polymerase beta is important for polymerization activity and fidelity. *Nucleic Acids Res. 35*, 2924–2935.
29. Sawaya, M. R., Prasad, R., Wilson, S. H., Kraut, J., and Pelletier, H. (1997) Crystal structures of human DNA polymerase beta complexed with gapped and nicked DNA: evidence for an induced fit mechanism. *Biochemistry 36*, 11205–11215.
30. Arndt, J. W., Gong, W., Zhong, X., Showalter, A. K., Liu, J., Dunlap, C. A., Lin, Z., Paxson, C., Tsai, M. D., and Chan, M. K. (2001) Insight inot the catalytic mechanism of DNA polymerase beta: structures of intermediate complexes. *Biochemistry 40*, 5368–5375.
31. Batra, V. K., Beard, W. A., Shock, D. D., Krahn, J. M., Pederson, L. C., and Wilson, S. H. (2005) Nucleotide-induced DNA polymerase active site motions accommodating a mutagenic DNA intermediate. *Structure 13*, 1225–1233.
32. Batra, V. K., Beard, W. A., Shock, D. D., Krahn, J. M., Pederson, L. C., and Wilson, S. H. (2006) Magnesium-induced assembly of a complete DNA polymerase catalytic complex. *Structure 14*, 757–766.

BI702104Y